PERKIN 2

The molecular structure of *N*,*N*′-diformohydrazide from *ab initio* studies (MP2 and density functional theory) and FTIR matrix spectroscopy

Luigi Bencivenni,[a] **Stella Nunziante Cesaro,**[b] **Maurizio Spoliti**[b] **and Fabio Ramondo** *[,c]

[a] *Istituto Nazionale di Fisica della Materia and* [b] *Dipartimento di Chimica, Università di Roma 'La Sapienza', I-00185, Roma, Italy*
[c] *Dipartimento di Chimica, Ingegneria Chimica e Materiali, Università dell'Aquila, I-67100 L'Aquila, Italy*

The FTIR spectrum of *N*,*N*′-diformohydrazide isolated in argon and nitrogen matrices is presented and discussed in terms of normal modes predicted by *ab initio* calculations. MP2/6-31G* and BLYP/6-31G* methods are applied to calculate vibrational frequencies, IR intensities and isotopic shifts of different structures of the molecule. The number of absorption bands and their frequencies for the isolated molecule differ significantly from those of *N*,*N*′-diformohydrazide in the solid state. The conformation of the undistorted molecule is different from the planar structure adopted by the molecule in the crystal and such a conformation change is proposed as the reason for the spectral differences. *Ab initio* calculations support this assignment and predict the vapour of *N*,*N*′-diformohydrazide to be a mixture of conformers.

Introduction

The rotational barrier heights about single bonds are very likely to be affected by intermolecular interactions. Appreciable structural discrepancies are often observed when gas-phase and condensed-phase molecules are compared and, as a consequence, the conformation of the isolated molecule may be different from that observed in crystal or solution.[1–5] *N*,*N*′-Diformohydrazide is an example of how the crystal field induces conformational changes. The crystal of *N*,*N*′-diformohydrazide consists of molecules close to being planar connected *via* strong NH···O=C hydrogen bonding.[5] The structure of the isolated molecule, never reported before to our knowledge, was determined, by *ab initio* molecular orbital calculations,[5,6] to be nonplanar at nitrogen and to show a twisted conformation about the N–N bond (C_2 symmetry). Simulations of the crystal field by *ab initio* calculations[6] revealed that hydrogen bonding occurring in the crystal is responsible for the conformational change.

Information about structural perturbations induced by crystal environment may also be derived from spectroscopic investigation. In the case of *N*,*N*′-diformohydrazide, the predicted conformational change[6] can readily emerge by comparing solid-state and gas-phase vibrational spectra. In fact one should expect quite a change in going from the C_2 point group (twisted conformer) of the isolated molecule to the centrosymmetric point group C_{2h} (planar conformer) of the crystal molecule. *N*,*N*′-Diformohydrazide possesses 24 fundamental vibrational modes described by 13A + 11B irreducible representations in the C_2 point group and $9A_g + 8B_u + 4A_u + 3B_g$ in the C_{2h} point group. On the basis of symmetry considerations, all the bands of the twisted conformations are IR active, whereas only 12 vibrations are expected to have IR activity in the case of centrosymmetric planar structures. Frequencies and band intensities, determined by *ab initio* methods,[6] indicate that the vibrational spectrum indeed changes with the molecular conformation.

The lack of experimental information for the gas-phase and the results evinced from the previous theoretical investigations[6] suggest that it is worthwhile looking for experimental infrared evidence about the conformation of the isolated molecule. The IR and Raman spectra of the crystal have been accurately studied[7] and for a proper comparison it is therefore essential to obtain the spectrum of the non-interacting molecule. Since rotational broadening of the bands in the vapour phase might complicate the analysis of the spectrum, it seems better to make use of matrix isolation. Moreover, it is known that some hydrazine derivatives may exist in the vapour as a mixture of conformers[8,9] and matrix isolation techniques could allow us to distinguish between different conformers present in the vapour phase as observed in the matrix spectrum of benzene-1,3,5-triol.[10] Therefore the FTIR spectra of *N*,*N*′-diformohydrazide and its *N*-deuterated isotopomers have been investigated in Ar and N_2 matrices. The conformation of the molecule is discussed on the basis of experimental and *ab initio* frequencies and isotopic shifts. Density functional theory (DFT) and Møller–Plesset perturbation theory (MP) methods are used for vibrational frequencies predictions. Both methods were found to be effective for predicting vibrational spectra of isolated molecules.[11,12]

Experimental

Commercial samples (Aldrich 98%) were purified by vacuum sublimation prior to the experiment and vaporized at *ca.* 350 K from a small glass oven located inside the vacuum chamber. The vapours coming from the molecular source were mixed with the matrix gas (argon or nitrogen) and deposited on a reflecting gold-plated copper cold-finger of a cryotip (202 CSA Air Products and Chemicals) at 12 K. Spectra were recorded by reflection using a Bruker IFS 113v interferometer. 200 scans were accumulated at 1 cm^{-1} resolution. High-purity nitrogen or argon (Caracciolo) were used as isolating gases. The gas flow-rate was generally regulated at 1 mmol h^{-1}.

The *N*,*N*′-deuterated species was prepared by repeated exchanges with D_2O.

Computational details

Ab initio molecular orbital calculations were run on an Alpha AXP-300/500 cluster of CASPUR c/o CICS at the University of Rome using the GAUSSIAN94 package.[13]

---

* Fax: 39-862-433753. E-Mail: framondo@axscaq.aquila.infn.it

Table 1 MP2/6-31G* torsional angles (degrees) of different structures of *N*,*N*′-diformohydrazide

	Configuration **I**			Rotational transition state **A**	Configuration **III** C_1	Rotational transition state **B**	Configuration **II** C_2[a]
	C_2 (**Ia**)[a]	C_2 (**Ib**)	C_2 (**Ic**)[b]				
∠C–N–N′–C′ (°)	65.5	148.8	110.5	103.9	78.2	110.4	107.2
∠H–N–N′–H′ (°)	137.3	160.8	179.6	−68.5	−101.2	−70.4	−73.1
∠N′–N–C=O (°)	16.4	8.9	14.4	9.0/61.3	7.8/161.2	60.5/169.4	171.5
∠O=C–N–H (°)	159.0	160.4	156.9	161.8/55.4	167.7/22.9	56.9/11.6	8.4
∠C′–N′–N–H (°)	−78.6	−6.0	−35.0	−138.5/−49.0	−59.6/−121.0	−47.3/−132.0	−89.9
∠N′–N–C–H (°)	−167.7	−174.1	−170.6	−173.1/−117.4	−173.7/−21.9	−118.4/−12.3	−9.9
∠H–N–C–H (°)	−25.0	−22.6	−28.1	−20.3/−125.9	−13.7/−160.2	−124.2/−170.2	−173.0

[a] Ref. 6. [b] Rotational transition state connecting the **Ia** and **Ib** stable conformations.

Table 2 Total energies (atomic units), relative stabilities, ΔE/kJ mol^{-1}, and zero-point energy corrections, ZPE/kJ mol^{-1}; of different structures of *N*,*N*′-diformohydrazide

	Configuration **I**				Transition state **A**	Configuration **III** C_1	Transition state **B**	Configuration **II** C_2[a]
	C_2 (**Ia**)[a]	C_2 (**Ib**)	C_2 (**Ic**)	C_{2h} (**Id**)[a]				
MP2/6-31G*	−337.608 36	−337.607 23	−337.606 71	−337.606 94	−337.576 99	−337.586 21	−337.580 98	−337.607 05
ΔE/kJ mol^{-1}	0.0	2.9	4.3	3.7	82.4	2.0	71.9	3.4
MP4[b] (f.c.)/6-31G*	−337.649 25	−337.647 42	−337.647 52	−337.646 70	−337.619 36	−337.648 52	−337.623 39	−337.647 86
ΔE^b/kJ mol^{-1}	0.0	4.8	4.5	6.7	78.5	1.9	67.9	3.6
MP4[b] (full)/6-31G*	−337.670 86	−337.669 14	−337.669 12	−337.668 38				
ΔE^b/kJ mol^{-1}	0.0	4.5	4.6	6.5				
ZPE/MP2/6-31G*/ kJ mol^{-1}	194.87	193.27	—	—	—	194.08	—	193.27
ZPE/BLYP/6-31G*/ kJ mol^{-1}	183.52	183.89	—	—	—	183.51	—	182.37

[a] Ref. 6. [b] MP4(SDTQ)/6-31G*//MP2/6-31G*.

The geometries of the investigated structures of *N*,*N*′-diformohydrazide were optimized within the appropriate symmetry constraints at the second-order of the Møller–Plesset perturbation theory[14] employing all the active orbitals, MP2(full), by the analytical gradient based technique. Harmonic vibrational frequencies were obtained by analytical second derivatives and dipole derivatives were calculated for the evaluation of the IR intensities.

Relative stabilities between different structures were evaluated by single-point energy calculations at the MP2 optimized geometries using the frozen core approximations at the fourth order of the Møller–Plesset perturbation theory, MP4(fc). The rotational barrier height about the N–N bond was also determined for the equilibrium structure including the core electrons, MP4(full).

MP2 vibrational frequencies were compared with the results of density functional theory calculations carried out employing the exchange-correlated functional of Becke[15,16] and Lee *et al.*[17] implemented in GAUSSIAN94 (BLYP). For MP2 and BLYP frequency calculations the split valence basis set 6-31G*[18] was used. The vibrational frequencies of the equilibrium structure were also evaluated employing the 6-311G** basis set.[18]

Results and discussion

Molecular conformation

Different structures have been studied in the present work. The previous paper[6] reported theoretical results of two configurations (**I** and **II** shown in Fig. 1) in which the formyl groups have been considered equivalent. In order to have a more detailed investigation of the potential energy surface, here we have taken into account an additional asymmetric configuration (C_1 point group), henceforth indicated as configuration **III** (Fig. 1). MP2/6-31G* geometry optimizations were carried out on this configuration without any symmetry constraint. Comparisons between the three structures reveal, once again, that the molecule prefers to adopt twisted geometries about the N–N bond and non-planar structures at nitrogen, irrespective of the relative orientation of the two formyl groups. Table 1 shows the torsional angles of each configuration. MP2/6-31G* frequency calculations revealed that all three twisted structures are true minima on the potential energy surface. From MP2/6-31G* and MP4/6-31G*//MP2/6-31G* energies (Table 2) it emerges that the configuration **I** is slightly favoured with respect to those reported as **III** (1.9 kJ mol^{-1}) and **II** (3.6 kJ mol^{-1}), although all the structures show a comparable stability. Table 3 reports the vibrational frequencies of the amide bands of each isomer along with the respective IR intensity bands. A quick

Table 3 MP2/6-31G* frequencies (ν/cm^{-1}) of the amide bands for **I**, **II** and **III** configurations of *N*,*N*′-diformohydrazide[a]

No.	Assignment[b]	**Ia**	**II**	**III**
ω_1	ν(N–H) (**B**)	3632 [77]	3596 [31]	3438 [48]
ω_2	ν(N–H) (**A**)	3624 [16]	3590 [43]	3555 [30]
ω_5	ν(C=O) (**A**)	1842 [169]	1827 [13]	1831 [262]
ω_6	ν(C=O) (**B**)	1812 [217]	1837 [569]	1815 [197]
ω_7	δ(N–H) (**A**)	1564 [59]	1502 [15]	1533 [96]
ω_8	δ(N–H) (**B**)	1494 [99]	1502 [6]	1494 [10]
ω_{11}	ν(C–N) (**A**)	1332 [34]	1360 [21]	1338 [30]
ω_{12}	ν(C–N) (**B**)	1136 [101]	1248 [270]	1236 [108]
ω_{16}	δ(NCO) (**B**)	914 [3]	760 [0]	869 [12]
ω_{17}	δ(NCO) (**A**)	810 [80]	484 [5]	598 [42]
ω_{18}	γ(N–H) (**A**)	572 [219]	611 [73]	684 [167]
ω_{19}	γ(N–H) (**B**)	459 [10]	546 [234]	529 [36]

[a] IR intensities (km mol^{-1}) are given in square brackets. [b] The symmetry of the modes is relative to the C_2 symmetry configurations (**Ia** and **II**).

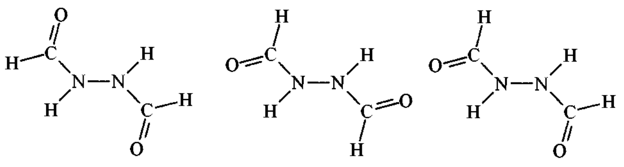

I II III

Fig. 1 Different configurations of *N*,*N*′-diformohydrazide

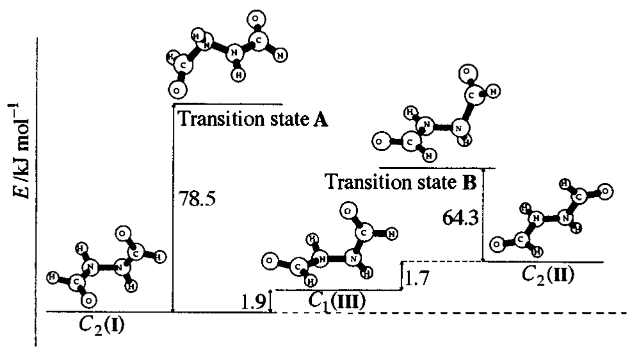

Fig. 2 C_2 and C_1 symmetry configurations of *N*,*N*′-diformohydrazide and the rotational transition states about the CN bonds. The energy values reported are calculated at MP4(fc)/6-31G*//MP2/6-31G*.

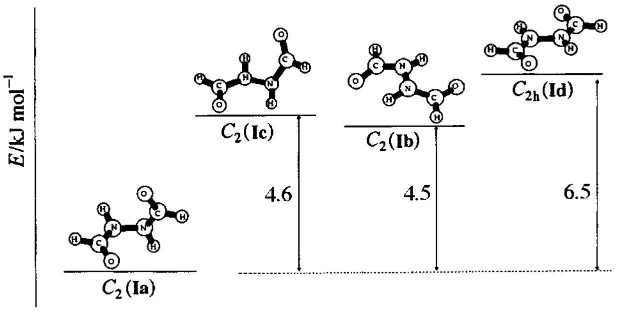

Fig. 3 The minimum conformations (**Ia** and **Ib**) of the **I** configuration of *N*,*N*′-diformohydrazide and the rotational transition state (**Ic**) connecting **Ia** and **Ib**. The energy values reported are calculated at MP4(full)/6-31G*//MP2/6-31G*.

scan of the theoretical spectra reveals that the three configurations are indeed spectroscopically distinguishable. Thus the spectral pattern observed in a low temperature matrix might be indicative of the presence of different isomers in the vapour. However, more reliable indications on the composition of the vapour phase can be inferred if we take into account the barrier heights to the torsion of the CN bonds. It can be easily seen from Fig. 2 that rotations about each CN bond allow passage from one configuration to another. In order to localize the transition states, MP2/6-31G* geometry optimizations were carried out with no symmetry constraints, thus finding two first-order saddle points (Fig. 2). The nature of each critical point was confirmed by the presence of one imaginary frequency, corresponding to the torsion about each CN bond. These torsional transition states connecting two different configurations are indicated, in Fig. 2, as **A** and **B**. MP2/6-31G* as well as MP4/6-31G* energies predict high torsional barrier heights about the CN bonds, in accordance with the considerable π-character of these bonds. The values of the torsional barrier heights (64 and 78 kJ mol^{-1}) suggest that there is a negligible chance that the molecule undergoes a change of configuration, at least at room temperature. The *ab initio* results, therefore, allow us to conclude that only one of the three configurations may exist in the vapour. In addition, since the spectrum is measured by vaporization of solid samples at *ca.* 320 K, we can reasonably suppose that the configuration of the formyl groups observed in our experiment is the same as adopted in the crystal, namely the **I** configuration.

Although changes of configuration from crystal to isolated molecules can be reasonably excluded, conspicuous conformational changes are instead expected[5,6] as a consequence of the strong intermolecular hydrogen bonding present in the crystal. Since distortions from planarity could be caused by rotation about the N–N bond and/or pyramidalization at nitrogen, it is interesting to explore accurately the potential energy surface in regions close to the planar structure. MP2/6-31G* geometry optimizations indicated the presence of a second, less stable minimum, corresponding to the structure shown in Fig. 3, differing from the C_{2h} one only by a slight nonplanarity at nitrogen atoms. Henceforth, we indicate such a structure as **Ib** and the equilibrium structure as **Ia** and we adopt for both of them the term conformation. The C_{2h} structure, characterized as a first-order saddle point and labelled in Fig. 3 as **Id**,[6] is therefore the transition state connecting two equivalent stable structures **Ib** (see Fig. 3). Moreover, the potential energy surface shows an additional first-order saddle point **Ic** corresponding to the transition state connecting the equilibrium structure **Ia** and the second stable structure **Ib**. On the basis of MP2/6-31G* frequency calculations we can therefore conclude that the configuration **I** of *N*,*N*′-diformohydrazide has two C_2 symmetry stable conformations of comparable stability (Table 2). Since MP2/6-31G* and MP4/6-31G* energies predict a very low barrier height to the conversion from **Ia** to **Ib** it is reasonable to suppose that the vapour is a mixture of both the conformations (**Ia** and **Ib**) of C_2 symmetry.

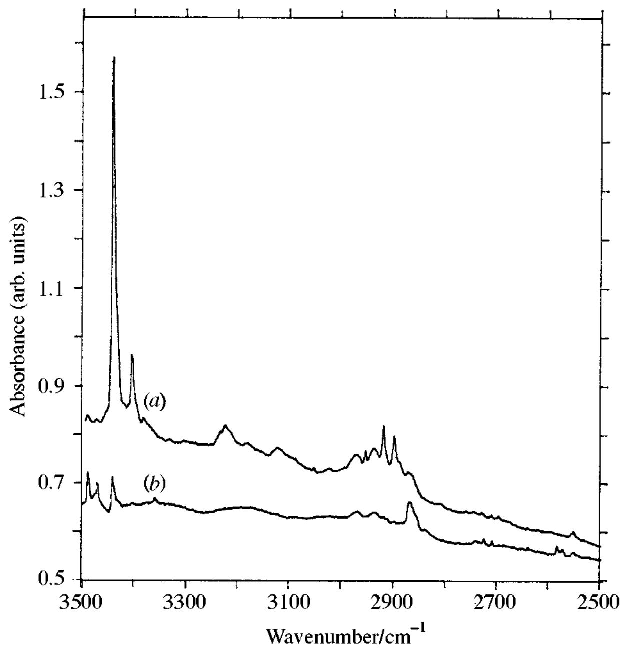

Fig. 4 The FTIR spectrum in the NH, ND, CH stretching region of *N*,*N*′-diformohydrazide (*a*) and of its *N*-deuterated species (*b*) in an argon matrix

Vibrational assignment

The FTIR spectra of *N*,*N*′-diformohydrazide and its *N*-deuterated isotopomer, measured in argon and nitrogen matrices from 4000–400 cm^{-1}, are presented in Figs. 4–6. Wavenumbers, intensities and assignments are summarized in Table 4, along with the vibrational spectra of the **Ia** and **Ib** conformations, as determined from MP2/6-31G* and BLYP/6-31G* calculations. The observed spectra and their assignments are discussed separately for each spectral region. The assignment of frequencies was based on the MP2/6-31G* and BLYP/6-31G* calculations of the wavenumbers, isotopic shifts and band intensities, although the predictions of the intensities do not always reproduce quantitatively the experimental spectra. For example, the intensities of the CH stretching modes are predicted to be one order of magnitude higher than those of the NH stretching modes, in clear contradiction with the observed bands (see Fig. 4). Basis sets larger than 6-31G* are often required for accurate intensity predictions; MP2/6-311G** frequency calculations were carried out on the equilibrium structure but we did not observe appreciable changes, as shown in Table 4. Nevertheless, the predicted intensities for different conformations have been considered in the assignment discussed in more detail below.

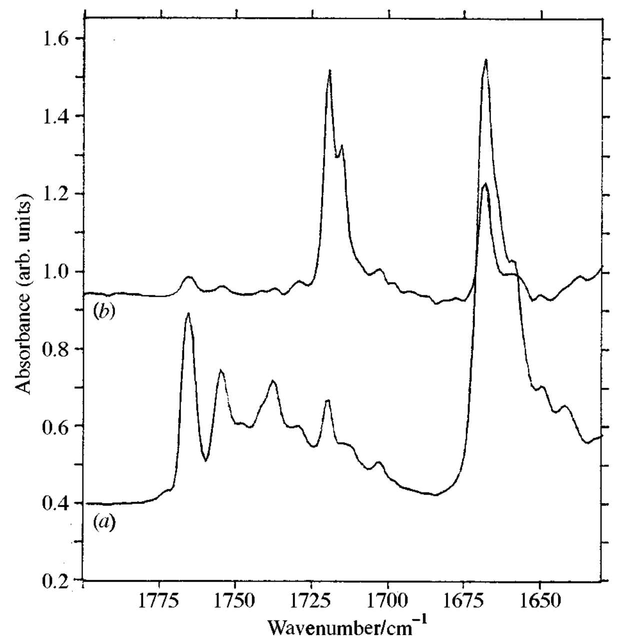

Fig. 5 The FTIR spectrum in the C=O stretching region of *N*,*N*′-diformohydrazide (*a*) and of its *N*-deuterated species (*b*) in an argon matrix

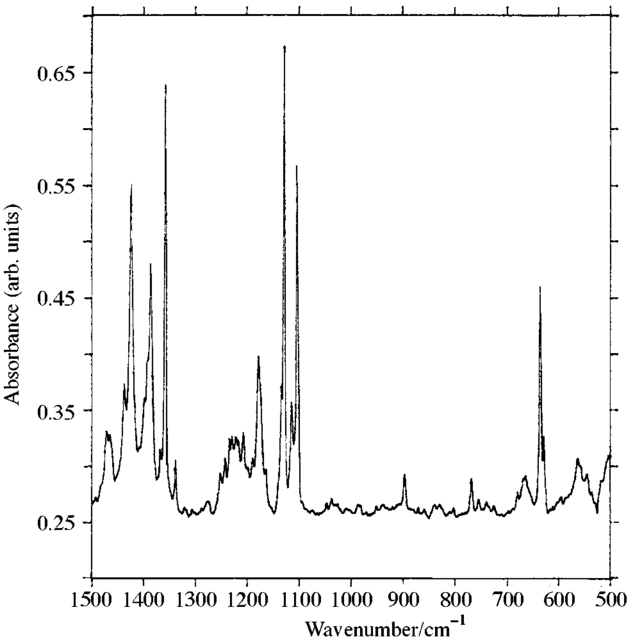

Fig. 6 The FTIR spectrum in the 1500–500 cm^{-1} region of *N*,*N*′-diformohydrazide in an argon matrix

3500–2000 cm^{-1} region. In the upper frequency region, shown in Fig. 4, we expect to observe the NH and CH stretching modes. A strong absorption band in fact appears in the ν(NH) region at 3440 cm^{-1} in argon and at 3428 cm^{-1} in nitrogen matrices in very close agreement with the wavenumbers of the ν(NH) modes calculated at the BLYP level. A weaker band is also measured at lower frequency, 3402 cm^{-1} (Ar) and 3420 cm^{-1} (N_2). The 3440/3402 and 3428/3420 band intensity ratios were found to be insensitive to matrix annealing suggesting that the observed splitting is due to an intrinsic property of the molecule rather than to a matrix-induced effect. The absence of temperature dependence also excludes the two bands originating in two different conformers, namely **Ia** and **Ib**, which are predicted to have significantly different *B* symmetry ν(NH) frequency modes. Considering the very low energy barrier separating the **Ia** and **Ib** conformers, the above ratio should change upon matrix annealing since the population of form **Ia** would increase with respect to that of form **Ib** in order to approach the equilibrium population ratio at the working temperature. The presence of two absorptions in the zone of the ν(NH) vibrations agrees much better with the spectrum predicted for the equilibrium conformation **Ia**, although the calculated intensity ratios of the asymmetric (*B*) and symmetric (*A*) stretching modes of 4.8 (MP2) and 10.3 (BLYP) do not fully agree with the experiment. The wavenumber difference between these two modes of 8 cm^{-1} (MP2) and 7 cm^{-1} (BLYP) is well reproduced by the 8 cm^{-1} observed in an N_2 matrix but it is far from that measured in an Ar matrix (40 cm^{-1}). Fig. 4(*b*) shows the spectrum in this region upon *N*-deuteration. The weak bands recorded at 2583–2580 cm^{-1} are assigned to ν(ND) modes. The observed isotopic shift (-840 cm^{-1}) is comparable with that expected from the *ab initio* force field (-940 cm^{-1}) if one considers that in our calculations anharmonicity corrections are not accounted for. The presence of a weak NH absorption at 3440 cm^{-1} suggests that deuteration is somewhat incomplete.

The CH stretching region exhibits a complex multiplet with weak components at 2968, 2958, 2934 and 2868 cm^{-1} and stronger absorptions at 2917 and 2897 cm^{-1} (Ar). A similar spectral pattern is observed in the nitrogen matrix with stronger absorptions at 2958 and 2933 cm^{-1} and weaker peaks at 2870, 2882 and 2915 cm^{-1}. The spectra change upon *N*-deuteration. The peaks at 2958, 2917 and 2897 cm^{-1} (Ar) disappear suggesting therefore that they can be assigned to combination bands of modes involving the NH group, such as (1668 + 1386) = 3054 cm^{-1}, (1668 + 1358) = 3026 cm^{-1}, (1460 + 1460) = 2920 cm^{-1}. All these wavenumbers come from the data obtained in the argon matrix and are not corrected for anharmonicity, therefore lower values would be more probable. Apart from these changes, the complicated spectral pattern of the ν(CH) region remains also for the *N*-deuterated species which shows one strong band at 2868 cm^{-1} along with two very weak absorptions at 2968 and 2934 cm^{-1}.

Although the assignment of this spectral region and, in particular, of the splitting of NH and CH stretching bands is clearly challenging and it would require more detailed work, there is clear evidence that matrix spectra are more crowded compared to those in the crystal phase. This leaves two possible interpretations: that the molecular conformation might be different from the planar centrosymmetric structure or, alternatively, that more than one species might be present in the matrix. *Ab initio* calculations suggest that each conformation **Ia** and **Ib** should give rise only to one ν(CH) absorption (see Table 4) at frequencies appreciably different from one another. Therefore, the simultaneous presence of both the conformers in the matrix could explain the appearance of split bands relative to the CH stretching.

1800–1600 cm^{-1} region. In this region we expect to observe the C=O stretching modes. According to normal coordinate analysis, the higher frequency mode, ω_5, is the symmetric ν(C=O) and the lower frequency mode, ω_6, is the out-of-phase ν(C=O). The argon matrix spectrum [Fig. 5(*a*)] shows a strong absorption at 1668 cm^{-1} with several weaker features at 1766, 1755, 1738 and 1721 cm^{-1}. In the nitrogen matrix the spectrum is similar with a strong band at 1663 cm^{-1} and weak absorptions at 1761, 1748, 1735 and 1714 cm^{-1}. From a close examination, it is possible to note that the stronger band is actually split into a doublet at 1668 and 1660 cm^{-1} (Ar) and at 1663 and 1658 cm^{-1} (N_2) and the intensity of the higher frequency components increases after sample annealing. In the Ar matrix spectrum of the deuterated compounds a different spectral pattern is observed with only two strong bands split into a doublet at 1720/1712 cm^{-1} and 1669/1660 cm^{-1}. The frequency of the stronger component coincides with the value measured for *N*,*N*′-diformohydrazide in accordance with the small isotopic shift (<5 cm^{-1}) predicted from *ab initio* calculations for the ν(C=O) modes. However, the intensity of the bands is found to

Table 4 *Ab initio* vibrational spectrum[a] of **Ia** and **Ib** conformers of CHO–NH–NH–CHO and IR experimental frequencies

		MP2/6-311G**	MP2/6-31G*		BLYP/6-31G*		Ar		N_2			
No.	Assignment	**Ia**	**Ia**	**Ib**	**Ia**	**Ib**	**Ia**	**Ib**	**Ia**	**Ib**		Crystal[b]
ω_1	ν(N–H) (**B**)	3658 [68]	3632 [77]	3617 [227]	3468 [31]	3467 [131]	3440		3428			2930s
ω_2	ν(N–H) (**A**)	3651 [16]	3624 [16]	3607 [1]	3461 [3]	3464 [1]	3402		3420			
ω_3	ν(C–H) (**A**)	3038 [0]	3072 [0]	3107 [0]	2874 [1]	2928 [0]	2968		2915			
ω_4	ν(C–H) (**B**)	3036 [175]	3071 [155]	3106 [114]	2873 [214]	2927 [158]	2934		2882			2920s
							2868		2870			
							2958[c]		2958[c]			
							2917[c]		2933[c]			
							2897[c]					
ω_5	ν(C=O) (**A**)	1840 [192]	1842 [169]	1819 [13]	1776 [156]	1731 [5]	1766		1761			
							1755[c]		1748[c]			
							1738[c]		1735[c]			
ω_6	ν(C=O) (**B**)	1808 [238]	1812 [217]	1767 [652]	1745 [285]	1680 [641]	1721	1668	1714	1663		1610vs
								1660[d]		1658[d]		
ω_7	δ(NH) (**A**)	1548 [61]	1564 [59]	1613 [0]	1488 [41]	1524 [0]	1460		1483			
									1470			
ω_8	δ(NH) (**B**)	1480 [84]	1494 [99]	1452 [251]	1423 [76]	1378 [182]	1428	1386	1432	1395		1480s
							1438[e]					
ω_9	δ(CH) (**A**)	1429 [2]	1439 [3]	1439 [0]	1379 [3]	1376 [0]						
ω_{10}	δ(CH) (**B**)	1424 [5]	1434 [4]	1415 [57]	1376 [5]	1350 [100]		1358		1363		1368vs
							1338[f]					
							1242[e]			1238[e]		
							1228[e]			1228[e]		
							1206[e]					
ω_{11}	ν(CN) (**A**)	1320 [30]	1332 [34]	1298 [0]	1213 [28]	1212 [0]	1177			1178		
ω_{12}	ν(CN) (**B**)	1115 [104]	1136 [101]	1191 [67]	1063 [108]	1113 [54]	1104	1128		1119	1141	1229s
							1114[f]					
ω_{13}	ν(N–N) (**A**)	1011 [0]	1026 [0]	1063 [1]	957 [1]	997 [0]	897[f]					
ω_{14}	γ(C–H) (**A**)	1045 [0]	1045 [0]	1003 [0]	980 [0]	925 [0]						
ω_{15}	γ(C–H) (**B**)	1019 [11]	1021 [5]	1013 [1]	958 [3]	940 [0]						800sh
ω_{16}	δ(NCO) (**B**)	915 [4]	914 [3]	785 [8]	856 [2]	743 [5]						753s
ω_{17}	δ(NCO) (**A**)	808 [67]	810 [80]	861 [12]	775 [46]	818 [5]	769					
							672[f]		673[f]			
ω_{18}	γ(N–H) (**A**)	548 [198]	572 [219]	472 [137]	507 [149]	474 [103]	635	563	637			
ω_{19}	γ(N–H) (**B**)	449 [9]	459 [10]	579 [32]	437 [7]	565 [13]						765m
ω_{20}	τ(C–N) (**A**)	409 [15]	410 [10]	319 [69]	371 [17]	283 [61]						
ω_{21}	τ(C–N) (**B**)	214 [40]	219 [42]	208 [51]	196 [33]	183 [47]						350sh
ω_{22}	δ(CNN) (**B**)	386 [2]	395 [3]	366 [61]	362 [2]	325 [25]						
ω_{23}	δ(CNN) (**A**)	178 [50]	183 [52]	255 [99]	162 [47]	240 [78]						
ω_{24}	τ(N–N) (**A**)	76 [2]	75 [3]	45 [5]	40 [6]	47 [2]						

[a] ω in cm^{-1}: IR intensities (km mol^{-1}) are given in square brackets. [b] Ref. 7; s = strong, vs = very strong, m = medium, sh = shoulder. [c] Combination band. [d] Matrix splitting. [e] Aggregates. [f] Unassigned.

change with *N*-deuteration as shown in Fig. 5(*b*). It is therefore evident that the overall pattern of this region is fundamentally different from that of the IR crystal spectrum.[7] The planar molecule in the crystal exhibits the asymmetric ν(C=O) at 1610 cm^{-1}, the only absorption measured in the IR spectrum, whereas the symmetric IR inactive mode occurs at 1675 cm^{-1} in the Raman spectrum.[7]

The complexity of the matrix spectra in this region could have different causes such as environmental effects, the presence of different molecular species, and Fermi resonance occurring between the strong carbonyl fundamentals and overtones or combination bands from the lower frequency modes. On the other hand, the absence of ν(NH) bands for dimers or oligomers, at least in a dilute matrix, allows us to exclude self-association in the matrix being responsible for some observed multiple bands. *Ab initio* results indicate that splitting of the ν(C=O) modes might arise from the simultaneous presence of both **Ia** and **Ib** conformers in the matrix. The calculated intensities suggest in fact that the asymmetric stretching should be very strong for both the conformers whereas the symmetric mode is predicted to be weaker for the **Ia** conformation and very small for the **Ib** conformation. On the grounds of theoretical results we propose therefore to assign the intense absorption at 1668 cm^{-1} to the *B* symmetry ν(C=O) of the **Ib** conformer. The shoulders observed at 1660 cm^{-1} (Ar) and 1658 cm^{-1} (N_2) are due to matrix site effects since they are lower upon annealing. Conformer **Ia** is expected to show the ν(C=O) modes very close to the bands observed at 1766 cm^{-1} (ω_5) and 1721 cm^{-1} (ω_6). The remaining weak absorptions, 1738 and 1755 cm^{-1}, can be assigned as combination bands of modes involving the NH group, (635 + 1104) = 1739 cm^{-1}, (635 + 1128) = 1763 cm^{-1}, since they are absent upon *N*-deuteration.

1600–800 cm^{-1} region. The spectrum in this region is presented in Fig. 6 and the assignment is summarized in Table 4. This spectral region is typical of some of the vibrations of the amide group, the δ(NH) mode (ω_7 and ω_8), the CN stretching with some contribution from δ(NH), (ω_{11} and ω_{12}), along with the δ(CH) (ω_9 and ω_{10}) and γ(NH) (ω_{18} and ω_{19}) vibrations. The MP2 and BLYP calculated spectra clearly indicate that the features of this region are indeed sensitive to the molecular conformation. For example, all δ(CH) modes are expected to be very weak with the exception of the *B* symmetry mode of the **Ib** conformer. For the latter one only the *B* symmetry δ(NH) and ν(CN) modes are predicted to be appreciably intense and to lie at frequencies well separated from the corresponding modes of the **Ia** conformer.

The spectra of *N*,*N*′-diformohydrazide show strong bands at 1428, 1386, 1358, 1177, 1128 and 1104 cm^{-1} (Ar) and at 1432, 1395, 1363, 1178, 1141 and 1119 cm^{-1} (N_2). Weaker absorptions are observed at 1460, 1338, 1114 and 897 cm^{-1} (Ar) and at 1483 and 1470 cm^{-1} (N_2). Finally, a complex multiplet (1242, 1228 and 1206 cm^{-1}), weakly present in the dilute matrix, increases its intensity with matrix concentration. On *N*-deuteration most of these absorptions are weakened and bands appear at 1465, 1381, 1346, 1242, 897, 860 and 833 cm^{-1}, although the peaks at 1465 and 897 cm^{-1} are already present but less pronounced in the spectrum of *N*,*N*′-diformohydrazide. Instead, only three strong infrared absorptions, at 1480, 1368 and 1229 cm^{-1}, are observed in this region for the crystal,[7] where the molecules arrange themselves in a conformation very similar to the **Ib** structure.

The matrix spectrum is indeed more crowded compared to the crystal phase and there is strong evidence that the free molecule does not possess a centrosymmetric planar structure. Although the band at 1435 cm^{-1} and the broad multiplet at *ca.* 1200 cm^{-1} can be assigned to dimer absorptions since they increase their intensity with matrix concentration or upon matrix annealing, most of the observed bands can be rationalized only by assuming the presence in the matrix of noncentrosymmetric conformers. On the grounds of our *ab initio* predictions, we assign the band at 1428 cm^{-1} to the δ(NH) mode (ω_8) of the equilibrium conformation. The corresponding mode of the *N*,*N*′-dideuterated isotopomer occurs at 1242 cm^{-1} with an isotopic shift (-186 cm^{-1}) in reasonable accordance with the value predicted from the *ab initio* forcefield, -205 cm^{-1} (MP2) and -209 cm^{-1} (BLYP). The equilibrium conformer is expected to show the δ(NH) mode (ω_7) very close to the weaker band measured at 1460 cm^{-1}.

The next strongest absorptions in the spectrum of *N*,*N*′-diformohydrazide at 1386 and 1358 cm^{-1} compare well with the BLYP wavenumbers calculated for the δ(CH) vibrations (1379 and 1376 cm^{-1}). The theoretical intensities for the equilibrium conformation, however, do not agree with the observed values since MP2 and BLYP calculations predict no significant absorptions in this region. A possible explanation of such a large discrepancy might be intrinsic in our method of calculation which provides accurate predictions of the wavenumbers but is still rather poor in reproducing some of the experimental infrared intensities. However a larger basis set, such as 6-311G**, does not solve the problem (see Table 4). Bending CH modes of appreciable intensity are expected only if the molecule adopts a conformation very close to the planar one, namely the **Ib** conformer. Therefore, if we assume that two conformations coexist in the matrix, we can assign the band at 1358 cm^{-1} to the δ(CH) mode (ω_{10}) and that at 1386 cm^{-1} to the δ(NH) vibration (ω_8) of the **Ib** conformation for the following reasons. Firstly, the BLYP frequencies of these modes, 1378 cm^{-1} (ω_8) and 1350 cm^{-1} (ω_{10}), are in excellent agreement with the experimental values; secondly, the spectrum measured upon *N*-deuteration shows a medium intensity absorption at 1380 cm^{-1} which correlates with the δ(CH) mode of *N*,*N*′-diformohydrazide. Since in a previous paper[6] some of us showed that hydrogen bonding occurring in the crystal does not produce measurable shifts in the δ(CH) frequencies, the correspondence of the δ(CH) modes in the matrix (1358 cm^{-1}) and the crystal IR spectrum (1368 cm^{-1}) is finally an important argument in favour of the chosen assignment. The ω_8 mode of the **Ib** conformer of CHONDNDCHO occurs at 1346 cm^{-1} with an isotopic shift (-40 cm^{-1}).

The simultaneous presence of the two conformers also explains the appearance of the doublets at 1128 and 1104 cm^{-1} (Ar) and 1141 and 1119 cm^{-1} (N_2). In fact, MP2 and BLYP intensity calculations indicate that each conformer should exhibit only one intense absorption, the *B* symmetry CN stretching, at frequencies close to the observed values (see Table 4). Moreover, the *ab initio* calculations indicate that the symmetric mode, ω_{11}, is expected at a much higher wavenumber than the antisymmetric mode, ω_{12}, in both conformations, namely 200 cm^{-1} (**Ia**) and 100 cm^{-1} (**Ib**). The splitting of the observed doublet is clearly much smaller (24 cm^{-1}), thus excluding the fact that the bands belong to the same molecular conformation. On the basis of these results, we assign the absorptions at 1104 and 1128 cm^{-1} to the **III** amide band of **Ia** and **Ib** conformers, respectively. The corresponding bands in the deuterated compounds still appear as a doublet occurring at 835 cm^{-1} (**Ia**) and 860 cm^{-1} (**Ib**). The predicted shifts downward upon *N*,*N*′-dideuteration are 185 cm^{-1} (**Ia** conformation) and 261 cm^{-1} (**Ib** conformation) whereas the observed values are 244 and 290 cm^{-1}.

Since *ab initio* calculations predict that the *A* symmetry ν(CN) should be appreciably intense when the molecule assumes the equilibrium structure, we assign the bands at 1177 cm^{-1} (Ar) and 1178 cm^{-1} (N_2) to this vibrational mode whose frequency is predicted at 1332 cm^{-1} (MP2) and 1213 cm^{-1} (BLYP). The corresponding band in the *N*,*N*′-dideuterated species is probably too weak to be observed.

800–500 cm^{-1} region. According to the *ab initio* spectra, we expected to find two bands of appreciable intensity in this region, namely the *A* symmetry δ(NCO), ω_{17}, and γ(NH), ω_{18}, vibrations. No appreciable absorption is instead predicted for the *B* symmetry vibrations laying in this region as well as both the γ(CH) modes. A strong and sharp band is observed in the argon matrix at 635 cm^{-1} and weak absorptions are found at 769, 665 and 563 cm^{-1}. Two weak bands are measured in a nitrogen matrix at 673 and 637 cm^{-1}. With the exception of the peak at 769 cm^{-1}, the remaining absorptions are significantly weakened in the spectrum of the *N*,*N*′-deuterated compound, thus suggesting that they have γ(NH) character. *N*-Deuteration also causes the appearance of a sharp and strong absorption at 516 cm^{-1} along with a weaker and broad peak at 525 cm^{-1}. Hence we assign the strong band at 635 cm^{-1} in the argon matrix to ω_{18}, γ(NH), for which the isotopic shift (-119 cm^{-1}) is consistent with the absorption at 516 cm^{-1} measured in the spectrum for CHONDNDCHO. The absorption at 769 cm^{-1} is assigned to the ω_{17} mode in excellent agreement with the BLYP value (775 cm^{-1}) whereas the weak band at 561 cm^{-1} is tentatively assigned to the γ(NH) mode of the less stable **Ib** conformer.

The last five vibrations, the δ(CNN) modes and the torsion vibrations about CN and NN bonds, are predicted to occur out of the range of our FTIR instrumentation.

Conclusions

It is quite clear that the overall pattern of the infrared spectrum of matrix isolated *N*,*N*′-diformohydrazide molecule is different from that of the crystal where the molecule is involved in strong hydrogen bonding. Clearly, the matrix isolated molecule is closer to the gas phase molecule for which quantum mechanical model calculations can be made. A good agreement between the observed frequencies and the MP2 and BLYP predictions is found when both twisted and quasi-planar conformations are considered. The existence of two minimum conformations of the most stable configuration, the same assumed by the molecule in the crystal, and the very low rotational barrier height about the N–N bond suggest that the vapour can be considered to be a mixture of conformers. The presence of both conformers in the matrix rationalizes some absorptions measured in the matrix and predicted from theoretical calculations.

Acknowledgements

The authors acknowledge financial support from the Faculty of Science of University of Rome 'La Sapienza' for the MURST contribution.

References

1 *Accurate Molecular Structures: Their Determination and Importance*, ed. A. Domenicano and I. Hargittai, International Union of Crystallography and Oxford University Press, Oxford, 1992.

2 R. G. Nanni, J. R. Ruble, G. A. Jeffrey and R. K. McMullan, *J. Mol. Struct.*, 1986, **147**, 369.

3 G. A. Jeffrey, J. R. Ruble, R. K. McMullan, D. J. DeFrees, J. S. Binkley and J. A. Pople, *Acta Crystallogr., Sect. B*, 1980, **36**, 2292.

4 G. A. Jeffrey, J. R. Ruble and J. H. Yates, *J. Am. Chem. Soc.*, 1984, **106**, 1571.
5 G. A. Jeffrey, J. R. Ruble, R. K. McMullan, D. J. DeFrees and J. A. Pople, *Acta Crystallogr.*, *Sect. B*, 1982, **38**, 1508.
6 F. Ramondo and L. Bencivenni, *J. Chem. Soc.*, *Perkin Trans. 2*, 1995, 1797.
7 P. Carmona and R. Lopez, *Spectrosc. Lett.*, 1982, **15**, 187.
8 K. Yamanouchi, M. Sugie, H. Takeo, C. Matsumura, M. Nakata, T. Nakata and K. Kuchitsu, *J. Phys. Chem.*, 1987, **91**, 823.
9 J. R. Durig and W. C. Harris, *J. Chem. Phys.*, 1971, **55**, 1735.
10 M. Spoliti, F. Ramondo and L. Bencivenni, *J. Mol. Struct.* (*THEOCHEM*), 1996, **390**, 139.
11 W. J. Hehre, L. Radom, P. v. R. Schleyer and J. A. Pople, *Ab Initio Molecular Orbital Theory*, Wiley, New York, 1986.
12 J. Florian and B. G. Johnson, *J. Chem. Phys.*, 1994, **98**, 3681.
13 M. J. Frisch, G. W. Trucks, H. B. Schlegel, P. M. W. Gill, B. G. Johnson, M. A. Robb, J. R. Cheeseman, T. Keith, G. A. Petersson, J. A. Montgomery, K. Raghavachari, M. A. Al-Laham, V. G. Zakrewski, J. V. Ortiz, J. B. Foresman, J. Cioslowski, B. B. Stefanov, A. Nanayakkara, M. Challacombe, C. Y. Peng, P. Y. Ayala, W. Chen, M. W. Wong, J. L. Andres, E. S. Replogle, R. Gomperts, R. L. Martin, D. J. Fox, J. S. Binkley, D. J. Defrees, J. Baker, J. P. Stewart, M. Head-Gordon, C. Gonzalez and J. A. Pople, GAUSSIAN 94, Gaussian Inc., Pittsburgh, PA, 1995.
14 C. Møller and M. S. Plesset, *Phys. Rev.*, 1934, **46**, 618.
15 A. D. Becke, *J. Chem. Phys.*, 1993, **98**, 5648.
16 A. D. Becke, *Phys. Rev. B*, 1988, **38**, 3098.
17 C. Lee, W. Yang and R. Parr, *Phys. Rev. B*, 1988, **37**, 785.
18 R. Poirer, R. Kari and I. G. Csizmadia, *Handbook of Gaussian Basis Sets*, Elsevier, Amsterdam, 1985.

Paper 7/00991G
Received 11*th February* 1997
Accepted 19*th May* 1997